Journal of Computers Vol. 31 No. 5, 2020, pp. 14-29
doi:10.3966/199115992020103105002

Research on Automatic Parking System Based on Multi-information Fusion

Chuan-wei Zhang*, Hong-jun Zeng, Meng-yue Yang, Jian-ping Wen, Man-zhi Yang

College of Mechanical Engineering, Xi'an University of Science and Technology, Xi'an Shaanxi 710054, China
{963923940, 1334817908, 1002443877, 120922284, 15029019244}@qq.com

Received 12 March 2019; Revised 29 July 2019; Accepted 28 August 2019

Abstract. Aiming at the requirement of automatic parking of intelligent vehicles in complex environment, this paper proposes an automatic parking method based on multi-information fusion. The method can not only improve the accuracy of the intelligent recognition of the parking space, but also ensure the safety and efficiency in the path planning process. The automatic parking system first uses multiple sensors to identify the relevant feature information of the surrounding environment of the parking space, and then calculates the output parking space recognition result according to the fuzzy inference system (FIS) and the two-way breadth-first search algorithm based on the rasterized map idea is used to carry out the corresponding path planning. Finally, the simulation analysis of the complex environment is carried out. The simulation results verify the rationality and effectiveness of the intelligent identification and parking path planning scheme. Then the self-developed automatic parking system was built in the experimental car for real test. The test results show that the correct rate of the parking system for automatic parking in complex environments is 89%-98%, with an average of 93.75%. The collision avoidance rate during the path planning process is 96% to 99%, and the average value is 98%, which verifies the good effect of the automatic parking method.

Keywords: automatic parking, multi-information fusion, parking space identification, path planning

1 Introduction

With the continuous growth of car ownership [1], it not only increases the traffic burden of the road surface, but also causes frequent traffic accidents and increased urban traffic congestion. In fact, the urban space is limited and the expansion is difficult. The crowded urban environment cannot provide enough parking spaces, irregular parking environment and narrow parking berths, resulting in "difficult parking" problems.

In this context, the automatic parking system began to appear [2]. According to the large data, the parking space recognition and path planning are very important for the automatic parking system [3]. At present, there are two main ways to realize the research on this subject at home and abroad. The first method: using multiple ultrasonic sensors for parking space detection, and then designing a control algorithm based on path planning. The advantage of this solution is that it can quickly obtain the location information of the current obstacles. Then, according to different algorithms, a geometric curve for the vehicle to perform autonomous parking is calculated. Finally, parking is carried out according to the constraints of the environment and the vehicles own motion control algorithm. Such as: Korean scholar Park et al [4]; Chinese scholar Tan Baocheng et al [5]; Chang Li University's Zhang Lili et al [6]. The second type of automatic parking scheme: using visual sensors for parking space detection, based on empirical control algorithms, using a variety of schemes (generally using neural networks or fuzzy logic). The aim is to change the parking in-place process in daily operation into a traditional control algorithm for controller operation, and to control the parking position of the vehicle according to the steering angle

* Corresponding Author

of the vehicle and the steering angle of the steering wheel. Such as: University of Cambridge, UK Ozkul et al [7], Taiwan's successful university Chao et al [8]; Heilongjiang University Long Zhaoxu et al [9].

However, there are the following problems in the above two parking space identification methods 1. The low intellectualization of automatic parking spot identification technology is all for automatic parking in fixed mode [10] (e.g. Vertical parking, horizontal parking). But in real life, due to the different driving level and parking habits of each driver, vehicles with different body attitude are parked on both sides of the target parking space. Irregular parking Spaces become common. The existing parking scheme cannot automatically park irregular parking Spaces, which makes it difficult to effectively utilize irregular parking Spaces.2. At present, there are many research methods for automatic parking road planning in China. However, for the complex environment with many obstacles, the traditional path planning [11] algorithm may not guarantee the safe driving of vehicles in the subsequent driving process, and the control algorithm is complex, real-time performance is not high, and the efficiency is low.

In order to improve intelligent degree of parking space identification and efficient safety of path planning in automatic parking process, this paper presents a method of automatic parking system based on multi - information fusion. The specific research contents are as follows: 1. Intelligent parking space recognition technology for complex scenes using multi-feature information. 2. Using the two-way breadth-first search algorithm of rasterized map idea to carry out more accurate path planning technology. 3. Verify the reliability and effectiveness of the design through the experimental vehicle. The research in this paper finally shows that the accuracy rate of automatic parking in complex environment is up to 89%~98%, with an average of 93.8%. Collision prevention rate in path planning is up to 96%~99%, with an average of 98%. Thus, the parking efficiency and safety performance of the vehicle in complex environment are improved, At the same time, it also realizes the reasonable utilization of irregular parking space resources.

2 The Principle of Automatic Parking System with Multiple Information Fusion

The principle of automatic parking system with multiple information fusion is shown in Fig. 1. In the process of finding the garage, the parking space sensing system of the experimental vehicle combines the characteristic data of the ultrasonic sensor, the visual information sensor and the speed sensor, obtains the spatial geometric parameters around the parking space, and introduces it into the parking space model. Five parking feature parameters are extracted as input of fuzzy inference until the identification result of the parking type is output. Finally, according to the raster map, the parking path planning module uses the bidirectional breadth-first search algorithm to achieve more accurate path planning matching. If the matching is successful, it will enter the parking state; if the matching is unsuccessful, the experimental car will continue to search for the garage. Ultrasonic sensors and camera sensors are installed on both sides of the experimental vehicle. Ultrasonic sensors are used to detect the length of the parking space. The camera sensor is used to identify the hub and parking line of the vehicle around the parking space. The speed sensor is used to read the speed of the vehicle and to travel the distance of the trolley. Fig. 2 is a simplified diagram of the automatic parking structure.

3 Parking Space Intelligent Identification Technology

3.1 Parking Space Model

In order to more realistically simulate the parking environment in complex situations. As shown in Fig. 3, it is assumed that there are two typical car body postures that are irregularly parked around the target parking space C, which are called A car tilted to the right and B car tilted to the left, and obstacles D of different sizes. According to the relative positional relationship between A car, B car, obstacle D and experimental car, the ultrasonic sensor and the camera sensor are used to perform one-way continuous scanning on the right side space of the experimental vehicle, and the vehicle body postures of the A and B vehicles and the obstacle D feature data are extracted, thereby establishing a parking space model.

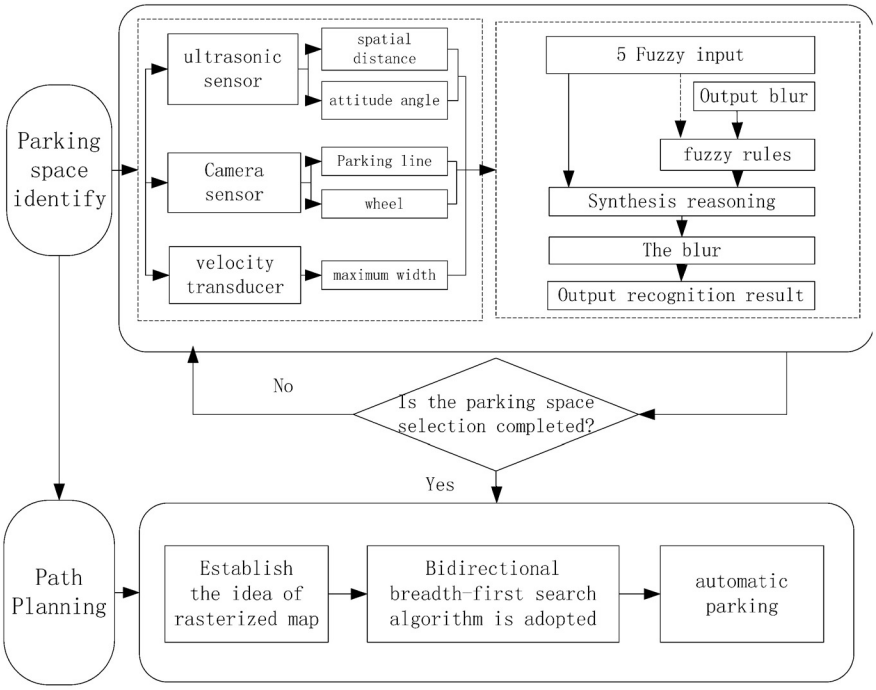

Fig. 1. Principle of automatic parking system with multiple information fusion

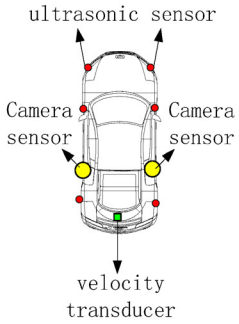

Fig. 2. The simplified diagram of the automatic parking structure

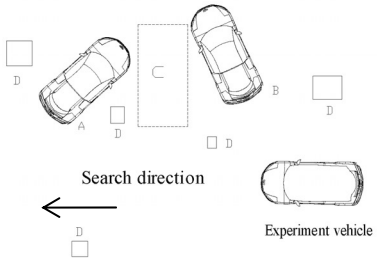

Fig. 3. Parking environment in complex conditions

3.2 Establishment of Vehicle Attitude Model and Extraction of Characteristic Parameters

There are three types of hierarchical models for information fusion, namely, low-level integration of information, middle-level fusion of features, and high-level integration of decision-making. In this paper, the middle-level fusion of feature information is used to extract the features collected by multi-sensors, and then the extracted information is analyzed and processed. The main fusion information includes: distance information detected by the ultrasonic sensor, mileage information obtained after the speed sensor is measured by the speed, camera sensor identification hub (with or without) and parking line

information (with or without), and extraction of the vehicle attitude angle α, As shown in Fig. 4, Two typical attitude vehicles A and B are modeled mathematically. And extract the space parameters a, b, c of the vehicle body and attitude angle α.

Fig. 4. Two typical attitude vehicles A and B

Let the coordinates of points a1, b1, c1, a2, b2, and c2 respectively is (X_{a1},Y_{a1}), (X_{b1},Y_{b1}), (X_{c1},Y_{c1}), (X_{a2},Y_{a2}), (X_{b2},Y_{b2}) and (X_{c3},Y_{c3}). Where X and Y are the calculated mileage distance of the speed sensor and the depth distance detected by the ultrasonic sensor, respectively. According to the geometric operation, the attitude angle α of the two types of vehicle bodies can be respectively obtained. The formula is as shown in (1) and (2). The attitude angle of the class A vehicle have hub, and the attitude angle of the class B vehicle have no hub.

$$\alpha = \begin{cases} \alpha_1 = \arctan\dfrac{|Y_a - Y_b|}{X_a - X_b} (, \text{Class A vehicle attitude angle, with hub .} & \textbf{(1)} \\ \alpha_2 = \pi/2 + \arctan\dfrac{|Y_a - Y_b|}{X_a - X_b}, \text{Class B attitude angle, no hub.} & \textbf{(2)} \end{cases})$$

Then, the horizontal width L_wide of the parking space is extracted, that is, the difference between the mileage values corresponding to the point c2 and the point a1, and the calculation formula is:

$$L\_wide = X_{c2} - X_{a1}. \tag{3}$$

When L_wide=0, the car A overlaps with the car B. Based on the safety principle, it is considered that the parking space cannot extract the space model. The ultrasonic information, the odometer information, the A vehicle body attitude angle α1, and the B body attitude angle α2 are combined to obtain the shortest space distance L_distance between the A car and the B car, as shown in (4):

$$L\_dis\tan ce = \min[L_{A-B}, L_{B-A}]. \tag{4}$$

Where L_{A-B} is the shortest distance from the a1 point of the A car to the b2c2 line of the B car, L_{B-A} is the shortest distance from the b2 point of the B car to the a1b1 line of the A car. According to the point-to-line formula, the following formula (5) (6) can be obtained:

$$L_{A-B} = \frac{\left[X_{a1} \bullet \tan\alpha_1 - Y_{a1} + Y_{b2} - X_{b2} \bullet \tan\alpha_2\right]}{\sqrt{1 + (\tan\alpha_2)^2}}. \tag{5}$$

$$L_{B-A} = \frac{\left[X_{b2} \bullet \tan\alpha_1 - Y_{b2} + Y_{a1} - X_{a1} \bullet \tan\alpha_1\right]}{\sqrt{1 + (\tan\alpha_1)^2}}. \tag{6}$$

The information collected by the camera is subjected to Equalize equalization image, adaptive binarization and morphological processing, and then Edge filtering detection, shape detection, and geometric matching are performed. Finally, the feature information of the parking line is optimized in the parameter space to obtain the recognition result.

3.3 Parking Type Recognition Based on Fuzzy Reasoning

Fuzzy logic has replaced traditional technical fuzzy sets in system engineering applications to process inaccurate data or information. In this paper, the Mamdani-type fuzzy reasoning method [12] is selected, and the five parameters extracted by the parking space model are used as inputs, The body attitude angle of A car is α1, the body attitude angle of B car is α2, the horizontal width of parking space is L_wide, and the shortest distance between A car and B car is L_distance. The driver's experience is judged as a benchmark rule, and the type of parking space is identified by inference calculation. Taking into account the geometric constraints of the parking warehousing path, the parking spaces are divided into three categories: horizontal parking spaces, vertical parking spaces, and irregular parking spaces. The fuzzy subsets of the input variables α1 and α2 are divided into three levels: {small, medium, large}, abbreviated as {S, M, L}, and the domain is [0, π]. The fuzzy subset of L_wide is divided into three levels: {short, medium, and long}, abbreviated as {S, M, L}, and the domain is $[0,+\infty]$. The fuzzy subset of L_distance is divided into 2 levels: {short, long}, abbreviated {S, L}, and the domain is $[0,+\infty]$. The fuzzy subset of the output variable parking space type is divided into 4 levels: {not parking space, horizontal parking space, vertical parking space, irregular parking space}, abbreviated as {not, Level, vertical, Irregular}, the domain is $[0,+\infty]$. The fuzzy set is completely characterized by its membership function [13], which can be described by a mathematical formula. Commonly used membership functions are triangle functions, trapezoidal functions, Gaussian functions, and Gbell functions. The membership functions of the input and output variables are all commonly used trapezoids. As shown in Fig. 5. W_car is the width of the experimental car, and L_car is the length of the experimental car.

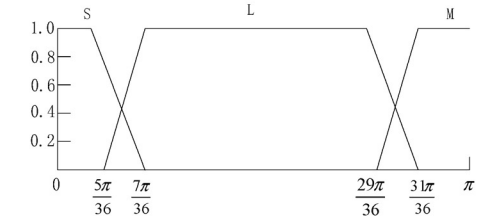

(a) Domain of α1

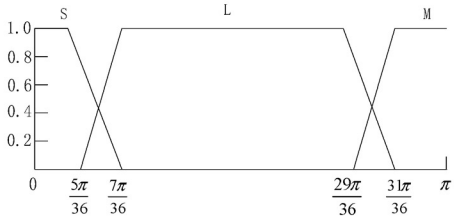

(b) Domain of α2

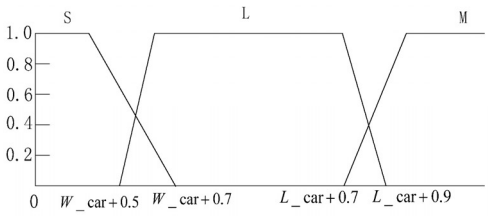

(c) Domain of L_wide

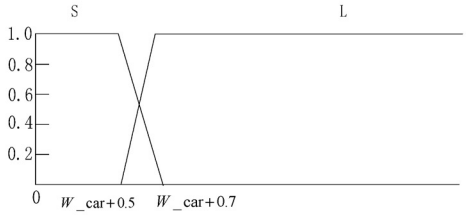

(d) Domain of L_distance

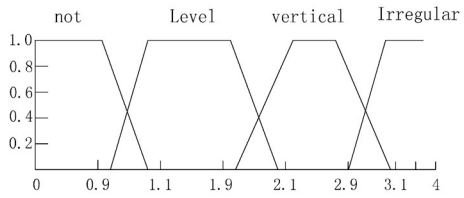

(f) Domain of parking space type

Fig. 5. Corresponding membership function

The form of the fuzzy rule library is: if $(\alpha_1)_i$ and $(\alpha_2)_i$ and $(L\_dis\tan ce)_i$ and (Parking line) and $(L\_wide)_i$ then $(iType)_i$, L, i = 1, 2... M, M is the total number of fuzzy rules. After the system model is established, according to the membership function relationship between input and output, combined with the driver's prior knowledge, 45 fuzzy rules as shown in Table 1 are finally determined.

Table 1. Fuzzy rules

number	α1	α2	L_wide	L_distance	Parking line(Y/N)	Result
1	L	L	L	L	Y	Level
2	L	L	L	S	Y	Level
3	L	L	M	L	Y	not
4	L	L	M	S	Y	not
5	L	L	S	L	N	not
6	L	L	S	S	Y	not
7	L	M	L	L	Y	Level
8	L	M	L	S	Y	not
9	L	M	M	L	Y	vertical
10	L	M	M	S	Y	vertical
11	L	M	S	L	Y	Irregular
12	L	M	S	S	Y	not
13	L	S	L	L	Y	Level
14	L	S	L	S	Y	Level
15	L	S	M	S	N	not
16	M	L	L	L	Y	Level
17	M	L	L	S	Y	Level
18	M	L	M	L	N	not
19	M	L	M	S	Y	vertical
20	M	L	S	L	Y	Irregular
21	M	L	S	S	N	not
22	M	M	L	L	Y	vertical
23	M	M	L	S	N	not
24	M	M	M	L	Y	vertical
25	M	M	M	S	Y	vertical
26	M	M	S	L	Y	Irregular
27	M	M	S	S	N	not
28	M	S	L	L	Y	Level
29	M	S	L	S	Y	Level
30	M	S	M	S	Y	vertical
31	S	L	L	L	N	not
32	S	L	L	S	Y	Level
33	S	L	M	L	N	not
34	S	L	M	S	N	not
35	S	L	S	L	N	not
36	S	L	S	S	Y	Level
37	S	M	L	L	Y	vertical
38	S	M	L	S	N	not
39	S	M	M	L	Y	vertical
40	S	M	M	S	Y	vertical
41	S	M	S	L	Y	Irregular
42	S	M	S	S	Y	not
43	S	S	L	L	N	not
44	S	S	L	S	Y	Level
45	S	S	M	S	Y	not

The establishment of the above fuzzy rules is mainly based on three principles: (1) When L_distance≥L_car+0.8, the necessary conditions for parallel parking parking planning are met. (2) When L_wide≥L_car+0.6, the necessary conditions for meeting the parking plan of the vertical parking space are met. (3) When L_distance≥L_car+0.6, the necessary conditions for irregular parking path planning are met.

4 Two-way Breadth-first Search Algorithm for Rasterized Map Ideas

4.1 Establishment of Rasterized Map

The rasterized map needs to be established before the path planning. The significance of the rasterized map is to discretize and blur the environmental information of the vehicle and surrounding obstacles and garages. Before the design of the shortest path algorithm for the vehicle, there must be a directed acyclic graph. The directed acyclic graph represents the distance relationship between the coordinate points in the current iteration and the coordinate points in the next decision phase. The rasterized map is shown in Fig. 6, where red represents the location of the map occupied by the vehicle itself, blue represents the location information of the garage, white represents the space area in which the vehicle can operate, and yellow represents obstacle information.

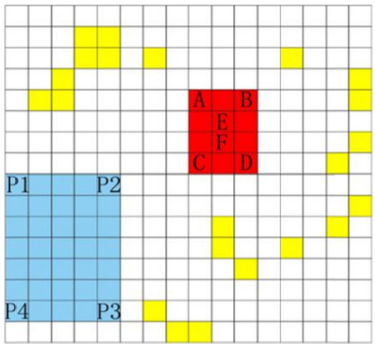

Fig. 6. Schematic diagram of rasterized map

The size of the grid is determined by the overall performance of the environment-aware system and the vehicle-mounted main controller. From the perspective of the effect, the more the number of grids, the better the effect. Assume that the parking space and the vehicle are two rectangular areas. The geometric relationship after parking is shown in Fig. 7:

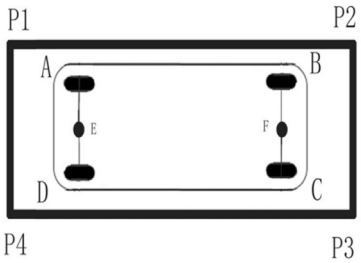

Fig. 7. Diagram of the relationship between vehicles and parking spaces

It can be seen from Fig. 7 that the four vertices of the parking space are represented as clockwise directions as P1, P2, P3, and P4, and their coordinates are defined as points P1(px1, py1), P2(px2, py2), (px3, py3) and P4 (px4, py4) respectively. From the perspective view of the car, the four vertices are represented as A, B, C, and D in a clockwise direction, and their coordinates are defined as A (ax, ay), B (bx, by), C (cx, cy), D (dx, dy). Let (the middle point of the front wheel axle) (x_f, y_f) have the coordinate (x_r, y_r), (the midpoint of the rear wheel axle) the F coordinate is w_d, the vehicle width is M, and the axle is h_m. From the perspective of fuzzy control, the midpoint motion of the front and rear wheels can be regarded as the trajectory of the whole vehicle. The half of the vehicle width $w_d/2$ and the half of the axle distance $h_m/2$ are used as the important basis for judging the boundary conditions. A set of formulas to satisfy parking success is shown in (7):

$$\begin{cases} x_r \in [px1..px2], y_r \in [py1..py2]. \\ ax \in [px1..px2], bx \in [py1..py2]. \\ \quad x_r \approx \lfloor | px2 - px1 | / 2 \rfloor. \\ \quad y_r \approx \lfloor | py2 - py1 | / 2 \rfloor. \\ x_f \in [px3..px4], y_f \in [py3..py4]. \\ cx \in [px3..px4], dx \in [py3..py4]. \\ \quad x_f \approx \lfloor | px4 - px3 | / 2 \rfloor. \\ \quad y_f \approx \lfloor | py4 - py3 | / 2 \rfloor. \end{cases} \tag{7}$$

When the four point coordinates A, B, C, and D of the vehicle are within the four point coordinates P1, P2, P3, and P4 of the garage, it is determined that the parking is successful. The entire path planning algorithm is based on the calculation of two points E and F. The moving process of point E and the relative direction information of points E and F are used as iteration inputs to analyze the path. Combined with the characteristics of the laboratory environment, the test yields a rasterized map. In the process of representing a rasterized map, the relationship of each lattice shown in Fig. 6 with respect to the vehicle is described in the form of two-dimensional data, which can be expressed by equation (8):

$$M_{ij} = \begin{cases} 0 \ \text{(Allow passage, white area).} \\ 1 \ \text{(No traffic allowed, yellow area)} \ (1 \le i \le n, 1 \le j \le m). \\ 2 \ \text{(Point E is at coordinates } i, j). \end{cases} \tag{8}$$

The array M_{ij} is the representation of the rasterized map, i represents the horizontal coordinate, and j represents the vertical coordinate. Each coordinate point is represented by a directed acyclic graph $G = (Dis, E, W)$, where Dis is the Manhattan distance [14] from each point to another point. In order to reduce the time complexity of the algorithm running and complete the update and search of the shortest route, this paper uses Manhattan distance instead of Euclidean geometry to express the distance between points. The correlation calculation is shown in formula (9):

$$\begin{aligned} & dis_{ijkl} = |i-k| + |j-l| (1 \le i \le n, \\ & 1 \le j \le m, 1 \le k \le n, 1 \le l \le m). \end{aligned} \tag{9}$$

The weighted array $\mathrm{dis_{ijkl}}$ represents the Manhattan distance from point (i, j) to point (k, l), and converts the weight formula into a two-dimensional array form, as shown in equation (10):

$$Dis_{j+i\times 10^{\lfloor \lg j \rfloor + 1}, k+l\times 10^{\lfloor \lg k \rfloor + 1}} = dis_{ijkl}. \tag{10}$$

The set E represents the relationship from each point to the neighboring point in the parking path process. The initialization of the relationship can be represented by a two-dimensional array, as shown in equation (11):

$$E_{ijkl} = \begin{cases} 1\{M_{ij} = 0 \wedge [(k = i-1 \wedge l = j-1) \vee (k = i+1 \wedge l = j+1), \\ \vee (k = i+1 \wedge l = j-1) \vee (k = i-1 \wedge l = j+1) \vee (k = i-1 \wedge l = j), \\ \vee (k = i \wedge l = j-1) \vee (k = i+1 \wedge l = j) \vee (k = i-1 \wedge l = j)] \wedge M_{kl} = 0.\} \\ 0 (\text{Other cases}) \end{cases} \tag{11}$$

The set of weight W represents the distance from the coordinates of the source point (point F) to the points (the sum of the weights). If the weight between the source point and the source point is initialized to 0, $E_{x_r y_r kl} = 1$ is satisfied near the source point, and k and l satisfy the coordinate relationship in the eight regions adjacent to the point F. Otherwise set it to ∞. In each iteration, the intermediate point is updated to obtain a new weight, and at the same time, the point set between each point and each point is updated, that is, the case of E. Therefore, for the initial weight set F, the condition of formula (12) needs to be satisfied:

$$F_{ij}=\begin{cases} Dis_{ij}(M_{i/10^{\lfloor(\lg\lfloor i\rfloor+1)/2\rfloor+1},i-10^{\lfloor(\lg\lfloor i\rfloor+1)/2\rfloor+1}}=0 \\ \wedge M_{j/10^{\lfloor(\lg\lfloor j\rfloor+1)/2\rfloor+1},j-10^{\lfloor(\lg\lfloor j\rfloor+1)/2\rfloor+1}}=0). \\ \infty(M_{i/10^{\lfloor(\lg\lfloor i\rfloor+1)/2\rfloor+1},i-10^{\lfloor(\lg\lfloor i\rfloor+1)/2\rfloor+1}}=1 \\ \vee M_{j/10^{\lfloor(\lg\lfloor j\rfloor+1)/2\rfloor+1},j-10^{\lfloor(\lg\lfloor j\rfloor+1)/2\rfloor+1}}=1). \end{cases} \quad (i\in[1..n], j\in[1..m]) \tag{12}$$

The directed acyclic graph established by equations (7)-(12) can be visually represented by graph (8), and graph (8) is the four cases where the size of the directed acyclic graph is intercepted under normal conditions.

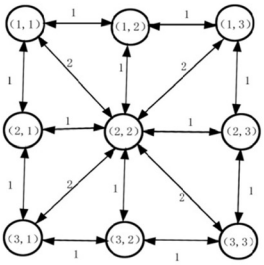

(a) General situation

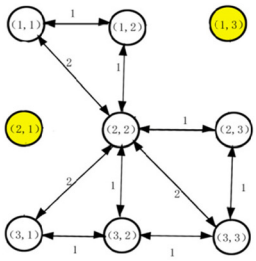

(b) Obstacle situation

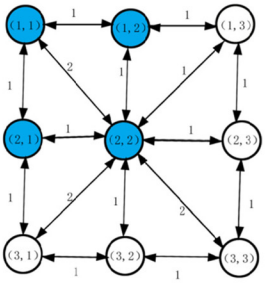

(c) Garage area situation

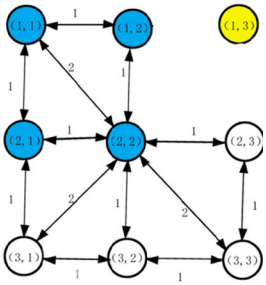

(d) Garages and obstacles situation

Fig. 8. A set of directed acyclic graphs for rasterized maps

Fig. 8(a) is a case of a directed acyclic graph when there is no barrier in the normal road surface and no garage area. The weight between any two points is 1 and the distance between the two points is 2 in Manhattan. When the vehicle is traveling in this area, it can travel freely, without doing other operations during the iterative process, and planning the path directly according to the shortest travel plan. Fig. 8(b) shows that there is an obstacle in the area, and the type of obstacle is not considered in the directed acyclic graph. Therefore, in the process of subsequent path planning, it is necessary to bypass the obstacle area to reach the target area. Fig. 8(c) shows that there is a target parking space in the area, and the vehicle fully enters the target parking space area, which means that the parking is successful. Therefore, the weight between the parking space area and other normal areas connected is the same as in Fig. 8(a). Fig. 8(d) belongs to the case where there is both a garage area and an obstacle. If the garage area in the acyclic chart is connected to the grid where the obstacle is located, it is the same as the processing in Fig. 8(b). The weight of the adjacent edge is set to ∞, and no update is performed in the subsequent decision algorithm. The above is the part of rasterized map creation and directed acyclic graph generation.

4.2 Two-way Breadth-first Search

Breadth-first search [15] is a more convenient algorithm in the graph theory algorithm. Unlike the depth-first search, its search process is very similar to the layer-by-layer traversal of the tree. In the scheme

adopted in this paper, after establishing the directed acyclic graph $G=(Dis,E,W)$, the algorithm is directly used in the two-dimensional array M_{ij} of the map. The set Dis is traversed layer by layer as the weight side set of this search scheme, and the initial coordinate of the point F in the rear axle of the vehicle is the starting point. According to the end condition in the formula (7), the breadth-first search is performed for the end condition of the search, and after obtaining the breadth-first search result, the optimal route planning scheme is obtained.

The two-way breadth-first search algorithm is designed to optimize and extend the breadth-first search algorithm, which means that search operations are performed at the same time from the source point and the end point. The algorithm ends when both traverse to the same or several intermediate points during the search. The two-part intermediate path mobility scheme is then combined by recursive operation to form the final overall path planning scheme. The schematic diagram of the algorithm for two-way breadth-first search is shown in Fig. 9:

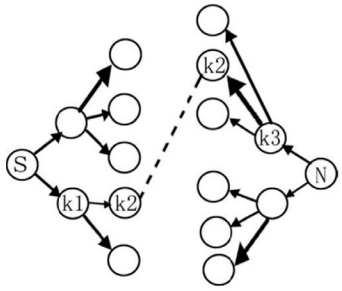

Fig. 9. Schematic diagram of two-way breadth-first search algorithm

The directed acyclic graph F formed in this paper, when performing the two-way breadth-first search, the starting point coordinate of the forward search is point G. The end point is that the coordinates of the starting point of the reverse search are the coordinate points in the blue area, and can be used as the forward search end point coordinate as long as the formula (7) is satisfied. However, during the running process, the algorithm can only select one point as the starting point for iterative operation. Therefore, in the special case of automatic parking, the optimal planning scheme is adopted for path planning (the case where the vehicle is just stopped at the center of the garage as the ending scheme). The starting point of the coordinates of the reverse search and the formula (13) are satisfied:

$$\begin{cases} Ex=\dfrac{px1+px3}{2}-\dfrac{(h_m+L_{end})\times\cos[\arctan(\dfrac{py2-py1}{px2-px1})]}{2}. \\ Ey=\dfrac{py1+py3}{2}-\dfrac{(h_m+L_{end})\times\sin[\arctan(\dfrac{py2-py1}{px2-px1})]}{2}. \end{cases} \tag{13}$$

The above indicates that the vehicle is just parked in the center of the garage. The midpoint of the line segment consisting of point E and point F coincides with the intersection of the rectangular diagonal lines formed by the projection of the garage on the plane, and the line segment EF is the same as the slope of the long side of the garage projection. In the adjacent two grids, in order to ensure the effective operation of the vehicle, in the process of each expansion, there are four directions of movement that can be considered, as shown in Fig. 10.

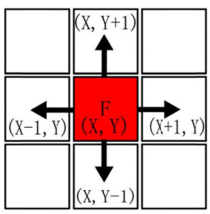

Fig. 10. Schematic diagram of the four moving directions of the rasterized map

As can be seen from Fig. 10, each decision takes into account four directions of movement during the process. Each movement of a grid represents an accumulation of 1 from the source point to the current total weight of the movement, thereby searching as an iterative weighting method. In order to ensure the effective execution of the two-way breadth-first search algorithm, it is first necessary to establish two queues, respectively storing a set Q_1 of all intermediate nodes from the source point to the end point. And storing a set Q_2 of all intermediate nodes from the end point (Ex, Ey) to the source point, respectively. The flow chart of the two-way breadth-first search process is shown in Fig. 11:

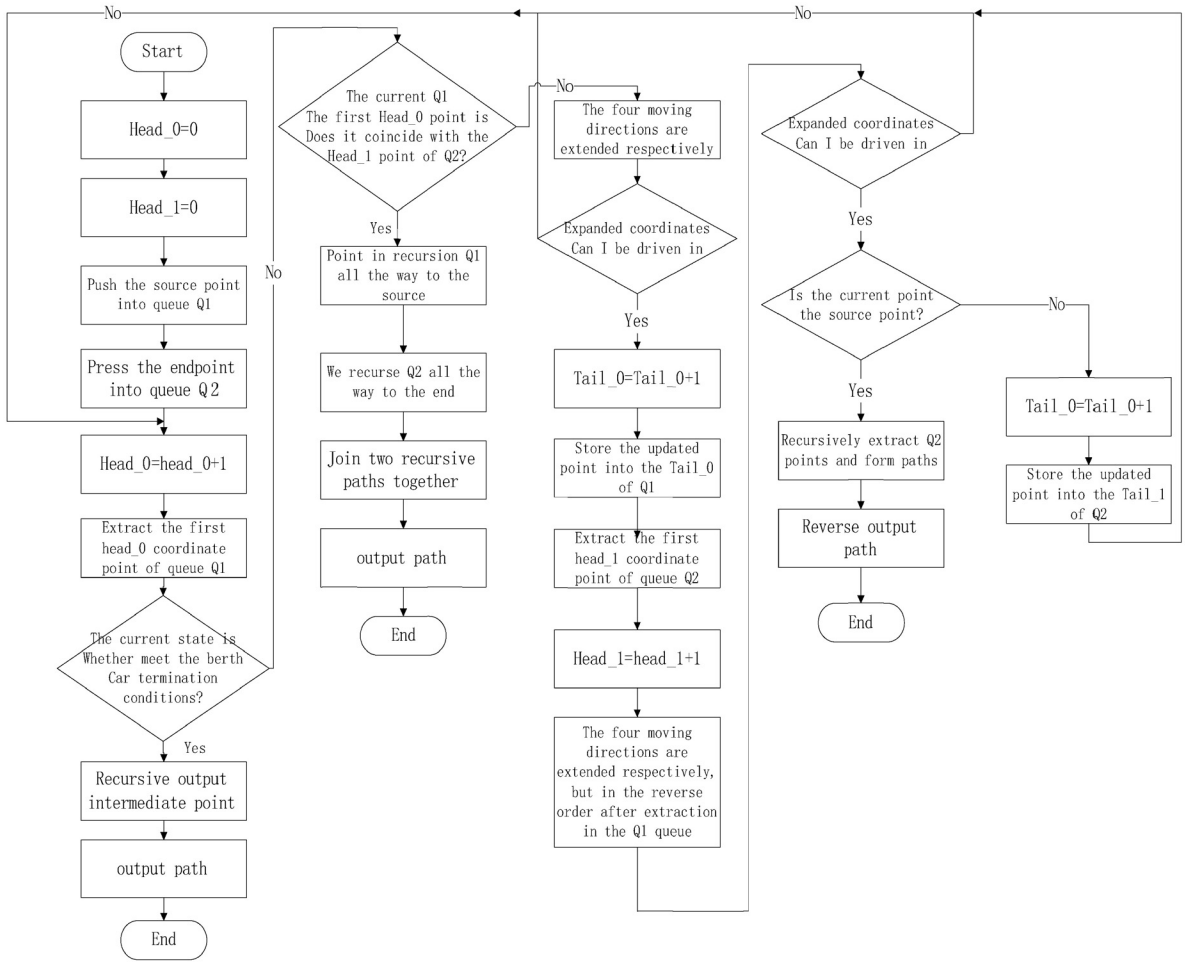

Fig. 11. Two-way breadth-first search flow chart

5 Experimental Results and Analysis

5.1 Two-way Breadth-first Search Performance Test under Different Conditions

For the two-way breadth-first search algorithm of this paper, the search performance test can be performed by dividing the finer raster map $(\mathrm{n,m})$. When $n=50, m=20$ and $n=60, m=30$, the bidirectional breadth-first search performance parameters can be obtained separately, as shown in Table 2:

Table 2. Two-way breadth-first search performance parameter table in two cases

Performance indicator project \ Different n and m	$n=50, m=20$	$n=60, m=30$
Step count	49	83
Number of generated grid nodes	269	401
Number of extended grid nodes	255	371
No initializer runtime (ms)	2.35	6.22

As can be seen from Table 2, the number of generated raster nodes indicates the total number of raster nodes generated by the two queues during the iteration process, which can reflect the time complexity and space complexity of the algorithm. The number of extended raster nodes represents the total number of nodes that are expanded. For example, when performing operations at each step, the number of nodes to be judged in the four directions to be considered can be used to judge the heuristic ability of the entire algorithm (for a certain case, the algorithm can generate the pros and cons of the path). Although the number of generated raster nodes is higher than the total number of steps, its runtime is within an acceptable range. Although the number of extended nodes is large, it is also within the acceptable range in rasterized maps. Therefore, to a large extent, this method can obtain the shortest path movement scheme. However, if the environment is special, different decision-making sequences in the search will cause different intermediate points to overlap, which will eventually lead to different steps.

The test in Table 2 uses a search from the source point in the order of "Up down left and right". Now the search order of each heuristic is changed to "Left right down up", "Right left up down", "Left up right down". The enlightenment order of the reverse search is opposite to the forward order, that is, "left" corresponds to "right" and "up" corresponds to "down". The test is also carried out under the premise of n=50 and m=20 and the conclusions are as shown in Table 3:

Table 3. Final steps of different heuristic orders

heuristic orders	Step count	Runtime(ms)
Up down left right	49	2.35
Left right down up	46	2.36
Right left up down	51	2.37
Left up right down	49	2.34

As can be seen from Table 3, different heuristic sequences lead to different conclusions, but there is almost no difference in each conclusion. Therefore, the bidirectional breadth-first search algorithm is used for path planning, and the optimal mobility scheme can be obtained.

5.1 Simulation Experiment

Before using the method of this paper for parking experiments, the establishment of rasterized maps must be completed. The most important part of map creation is to determine the values of n and m. Let the length of the experimental site be Col and the width be Cow. The length of the entire map is n and the width is m. Then, the segmentation of the rasterized map is performed, and the area represented by each raster is the area of $Col/n \times Cow/m$. Since the processor of this experimental platform has a lower main frequency and a smaller RAM, the following parameters are used in the experimental vehicle and the experimental field, as shown in Table 4:

Table 4. Experimental vehicle and experimental site parameter

project	Name	Parameters
Experimental site	Length (Col)	130 cm
	Width (Cow)	86 cm
Test Vehicle Parameters	Vehicle width (W_d)	17.8 cm
	Wheelbase (H_m)	19.4 cm
	vehicle length (L)	28.5 cm
	Front Wheel Shaft and Head Distance (L_{begin})	5.4 cm
	Distance between rear axle and rear axle (L_{end})	2.5 cm
	Minimum turning radius $(R_{\min})$	33.28 cm

According to Table 4, the minimum turning radius of the experimental vehicle is 33.28 cm. Assuming that the midpoint F of the rear axle moves in the middle of the grid (on the intersection of the diagonals) and can be turned to the middle of the grid point on the upper side, then if the side length of the grid is Ran, then there is $Ran \le 33.28cm$. The choice of n and m should satisfy the following relationship:

$$m \geq \left\lceil \frac{Cow}{Ran} \right\rceil, n \geq \left\lceil \frac{Col}{Ran} \right\rceil. \tag{14}$$

According to formula (14), $n \geq 4, m \geq 3$ can be obtained. Since $(\mathrm{n,m})$ is more subdivided, the selected system can withstand the largest $(\mathrm{n,m})$, and $2/3(\mathrm{n,m})_{\max}$ as the last value after testing. The values of n and m are: $n = 200, m = 150$. Each grid has a side length of $\max(Cow/n, Col/n)$ and an area of $\max^2(Cow/n, Col/n)$. In the plan view, the grid side length is 0.57 cm and the area is 0.3171 cm^2. As can be seen from Table (4), the experimental vehicle occupies a grid number of 5032 in the map, for a total of 1600 grid spaces.

In order to verify the reliability of the parking space intelligent identification technology and the correctness of the two-way breadth-first search algorithm for rasterized map ideas. The path planning simulation model is built by Matlab, and the center of the rear axle of the experimental car is taken as the center point of the path trajectory planning. The change results of the parking space parameters are observed for four different parking space scenes as shown in Fig. 12.

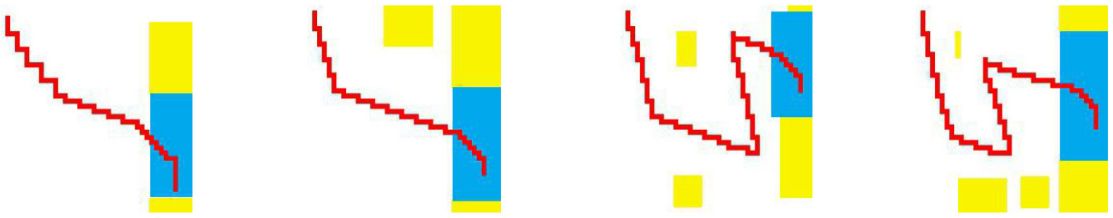

(a) Ideal situation (b) There are cars in front (c) Less obstacles (d) More obstacles

Fig. 12. Automated parking results of multiple information fusion algorithms in different environments

Table 5 is the statistical result of the simulation test. It can be seen from the simulation results that the parking space intelligent sensing system based on multi-information fusion can simulate the driver's thinking for parking space recognition. In the path planning process, complex obstacles can also be avoided, in accordance with the practical operating habits of skilled drivers.

Table 5. Results of simulation test

Serial number	α1	α2	L_wide	$(L\text{—\_distance})_i$	Lane line (with or without)	Desired output
(a)	π	π	36	36	with	Horizontal parking
(b)	π/2	π	38	38	with	Horizontal parking
(c)	2π/9	π/6	23	20	with	Irregular parking
(d)	3π/4	2π/3	22	21	with	Irregular parking

The parking space sensing technology can not only accurately identify irregular parking space scenes, but also output reasonable parking space types. The results show that the bidirectional breadth-first search algorithm based on rasterized map can accurately plan the parking path. The parking trajectory generated by the fitted parking path using mat lab is shown in Fig. 13.

Fig. 13 describes the parking simulation track diagram of the parking profile based on the path planning conclusion. After using cubic spline interpolation between each two grid path points, the vehicle steering Angle can be calculated according to the first derivative of the function, so as to control the vehicle parking operation. From Fig. 13(a) and Fig. 13(b), it can be seen that the parking path is a continuous curve under ideal conditions. For the two cases of Fig. 13(c) and Fig. 13(d), It doesn't fit directly from the starting point to the end point, Its trajectory is divided into three segments. Simulation results show that the sensing technology of the system can identify parking Spaces in complex environments and plan the safe parking path according to the parking space type. Multi-information fusion based parking space sensing technology can effectively improve the intelligent level of automatic parking sensing system, The bidirectional breadth-first search algorithm based on rasterized map can enhance the success rate of path planning.

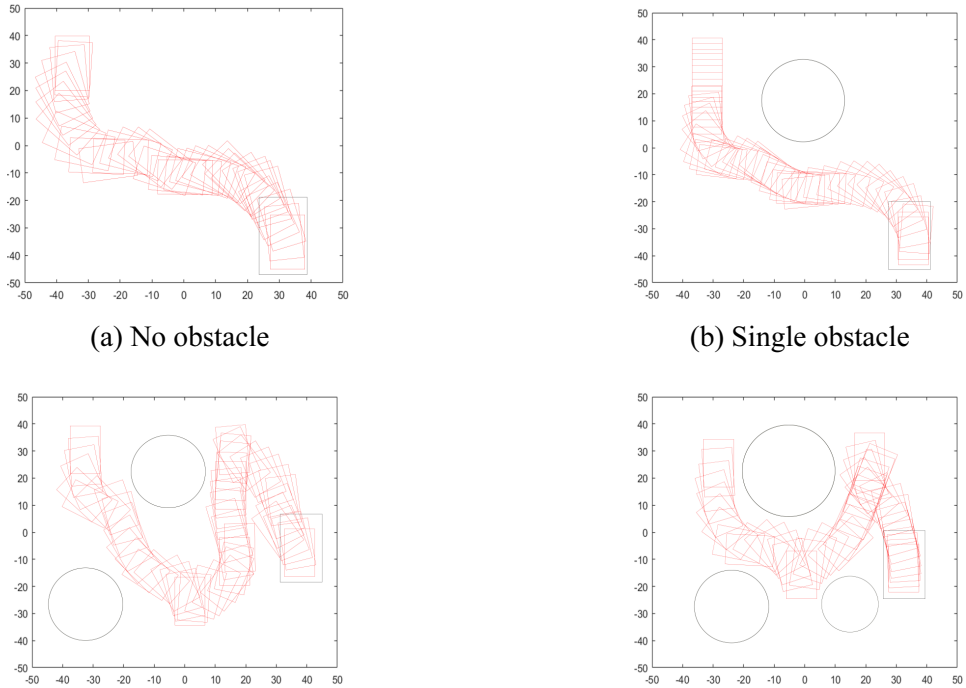

(a) No obstacle (b) Single obstacle

(c) Two obstacles (d) Multiple obstacles

Fig. 13. Vehicle contour parking simulation track diagram

5.3 Experimental Vehicle Test

For the parking space scene in complex environment, the traditional four-stage parking algorithm is used to write the experimental platform for experimental verification, and comprehensive comparison with the scheme of this paper. Such as: Fig. 14 ①-⑥ is automated parking experiments using multiple information fusions in complex environments. As can be seen from Fig. 14 ④⑤⑥, automatic parking can be completed even in an irregular parking space environment in which the surrounding obstacles are complicated and the body posture is different. As shown in Fig. 15, the traditional four-segment automatic parking experiment was used in the same complex environment. As can be seen from Fig. 15 ⑦⑧⑨, in a complex irregular parking environment, the traditional four-segment parking mode is prone to collision events and safe and effective automatic parking is not possible.

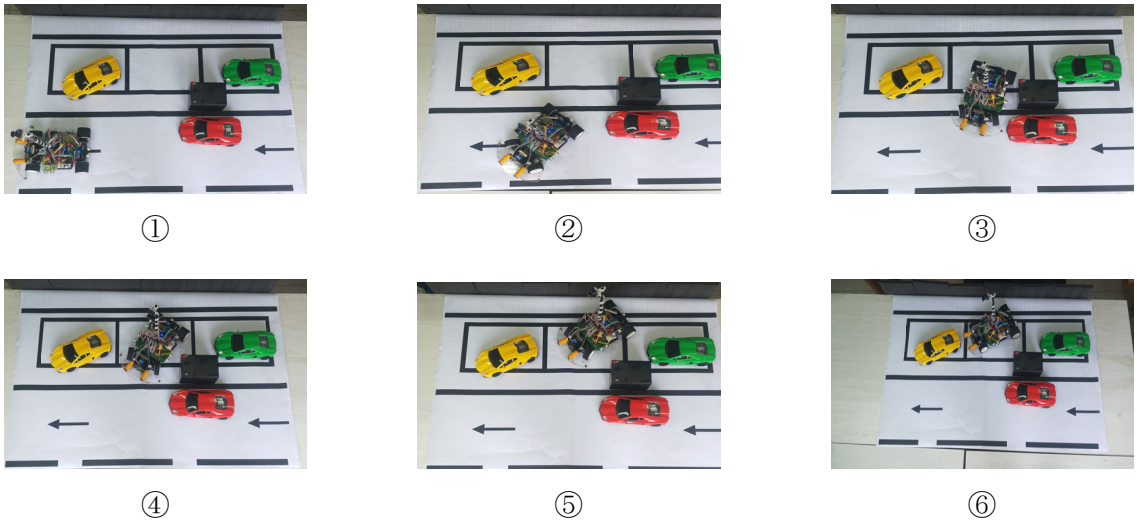

① ② ③

④ ⑤ ⑥

Fig. 14. Using an automated parking experiment based on multi-information fusion in a complex environment

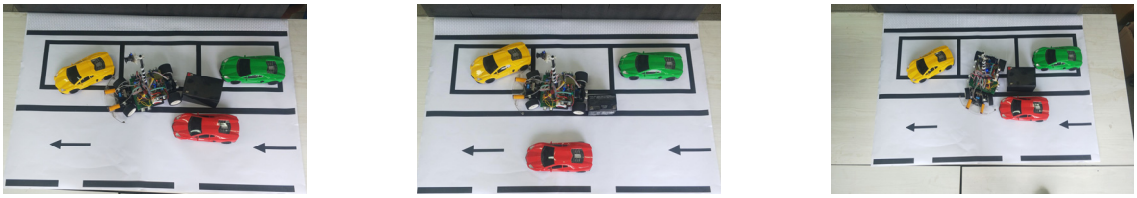

⑦ ⑧ ⑨

Fig. 15. Automated parking experiment results using a traditional four-segment parking algorithm in a complex environment

Then, the scene recognition is verified on the experimental vehicle, and the performance of the parking space sensing technology designed in this paper is evaluated by the accuracy of the recognition. According to the preset parking space scene, the experimental vehicle equipped with the automatic parking system is used for searching, and the parking controller performs path planning according to the type of parking space that is output in real time. After the path planning is successful, the actual parking space type is derived and compared with the expected parking space type. In the Table 6(a) to Table 6(d) scenario, 100 tests were performed respectively, and the accuracy was finally obtained. As can be seen from Table 6, the recognition accuracy in the (a)-(d) scenario is at least 89% and the highest is 98%. The highest collision avoidance rate during path planning is 99% and the lowest is 96%. The average accuracy and anti-collision rate are high, which indicates that the automatic parking system based on multi-information fusion designed in this paper performs well.

Table 6. Results of the test

Serial number	Desired output	Total number of trials	Correct recognition times	Accuracy (%)	Number of collisions	Collision rate (%)
(a)	Horizontal parking	100	98	98	1	1
(b)	Horizontal parking	100	96	96	1	1
(c)	Irregular parking	100	89	89	2	2
(d)	Irregular parking	100	92	92	4	4

6 Conclusion

In the complex environment, this paper uses the automatic parking method based on multi-information fusion to carry out theoretical analysis and simulation experiments, and can draw the following conclusions: (1)The directed acyclic graph of the established rasterized map can describe the complex parking space environment more completely. (2)Using fuzzy inference method for multi-sensor information fusion, the parking space recognition can effectively identify the rules and irregular parking spaces. (3)The two-way breadth-first search algorithm using rasterized map idea can carry out safer and more efficient path planning. It can be seen from the test results that the average recognition accuracy of the four scenarios tested can reach 93.75%, and the average collision avoidance rate can reach 98% during the path planning process. Therefore, the method can not only improve the accuracy of the intelligent recognition of the parking space, but also ensure the safety and efficiency of the path planning process. Due to the limitation of the experimental conditions, there is a certain gap between the experimental car and the real car in the treatment of the experimental link. Follow-up work can be carried out from the following aspects:

(1)Improve the upper computer system. For decision control algorithm, its dependence on environmental information is very high. In this paper, in order to reduce program errors and improve experimental efficiency, a series of upper computer programs will be written through VS2015 (including the upper computer program for data transmission to calibrate the position of vehicles and parking Spaces).

(2) This paper is a comparative experiment completed under the condition of experimental vehicle, In the future, the setting of individual steps and variables will be adjusted and studied when the driverless

experimental vehicle is built, and carry on the real car experiment.

Acknowledgements

This paper was supported by National Key R&D Program of China (2018YFC0808203) and Supported by Foundation of Shaanxi Key Laboratory of Integrated and Intelligent Navigation (SKLIIN-20180101), the authors would also like to express their deep gratitude for the support of the College of Mechanical Engineering, Xi'an University of Science and Technology.

References

[1] China Industry Information, 2018-2024 China automotive industry market evaluation and investment prospect evaluation report [EB/OL]. <http://www.chyxx.com/industry/201802/614688.html>, 2018.

[2] P.W. Zuo, Q.G Meng, Y. X. Li, Analysis of the development and prospects of automatic parking system [EB/OL]. <https://www.sohu.com/a/218255872_465591>, 2018.

[3] Park Chang-ho, etc. Design of Automatic Parking System, Science Press, 2014.

[4] W.J. Park, B.S. Kim. Parking space detection using ultrasonic sensor in parking assistance system, in: Proc. IEEE Intelligent Vehicles Symposium Eindhoven University of Technology Eindhoven, 2008.

[5] B.C. Tan, T. Ma, Research on parking guidance system based on Ultrasonic ranging, Electronic Design Engineering 23(18)(2015J) 96-99.

[6] L.L. Zhang, Research on automatic parking system based on Ultrasonic ranging, Chang'an University, 2017.

[7] T. Ozkul, M. Mukbil, S. Al-Dafri. A fuzzy logic based hierarchical driver aid for parallel parking, in: Proc. Artificial Intelligence Knowledge Engineering and Date BASES, 2008.

[8] C.H. Chao, C.H. Ho, Omni-directional vision-Based parallel-Parking control design for car-like mobile robot, in: Proc. 2005 IEEE International Conference on Mechatronics, 2005.

[9] Z.X. Long, C.X. Xing, M.X. Zhao, L. Luo, D.Y. Zhou, Research on automatic parking method based on active vision, Heilongjiang Science and Technology Information 18(2017) 156-157.

[10] H.J. Li, B. Gong, Analysis on the Technology and Application of automatic parking system, Journal of Huainan Vocational and Technical College 18 (5)(2018) 109-110.

[11] F. Ding, Research on an automatic parking system based on a four-stage path planning, Hefei University of Technology, 2014.

[12] Z.N. Shen, Research on automatic parking system based on multi-sensor information fusion, Jiangsu University, 2017.

[13] S.L. Li, X. Zhang, W.Y. Zhou, Research and simulation of automatic parking track based on fuzzy control, Computer Technology and Development 27(2)(2017) 163-166, 170.

[14] K.J. Zhu, J. Li. Background subtraction method for detecting moving targets in Manhattan range, Laser Journal 10(2017) 85-89.

[15] Y.H. Tan, Implementation of weight-first search algorithm based on weights in Jiugong Lattice, Fujian Computer 30 (3)(2014) 145-146.